H2Open Journal

IWA PUBLISHING

H2Open Journal Vol 6 No 2, 256 doi: 10.2166/h2oj.2023.068

Effects of a conical enlarging shaft on hydraulic performances of siphon-shaft spillways

M. Cihan Aydin and Ali Emre Ulu*

Department of Civil Engineering, Bitlis Eren University, Bitlis 13100, Turkey
*Corresponding author. E-mail: aliemreulu@gmail.com

MCA, 0000-0002-5477-1033; AEU, 0000-0001-7499-3891

ABSTRACT

Siphon-shaft spillways can discharge large amounts of water down to the crest level in a narrow reservoir thanks to the siphonic pressures. However, cavitational pressures in the siphon-shaft limit the operating head of these spillways. An enlargement at the shaft mouth can reduce the vacuum pressures and velocities within the siphonic flows, thereby removing the risk of cavitation occurring. In this study, four different enlarging shaft profiles with various coning angles of 0°, 10°, 15°, and 20° were applied to a siphon-shaft spillway model to eliminate cavitation pressures in the shaft. These models are analyzed in three dimensions by computational fluid dynamics based on the RANS turbulence model coupled with the Volume of Fluid (VOF) method to simulate fluid motion. The numerical uncertainties of the simulation were calibrated with some experimental results and techniques in the literature. The results showed that the enlargement in the shaft mouth with a conical profile significantly decreased the vacuum pressures and velocities in the siphon-shaft. Thus, the use of conical profiles considerably reduced the cavitation numbers along the shaft surface and increased the discharge performance by about 11%.

Key words: cavitation control, CFD, computational fluid dynamics, linear enlargement, shaft profile, siphon-shaft spillway

HIGHLIGHTS

- A new methodological and hydraulic approach to siphon-shaft weirs is presented.
- The models applied in the study significantly reduced the cavitation pressure.
- With the applied models, the spillway performance of the siphon-shaft weirs has been significantly improved.

GRAPHICAL ABSTRACT

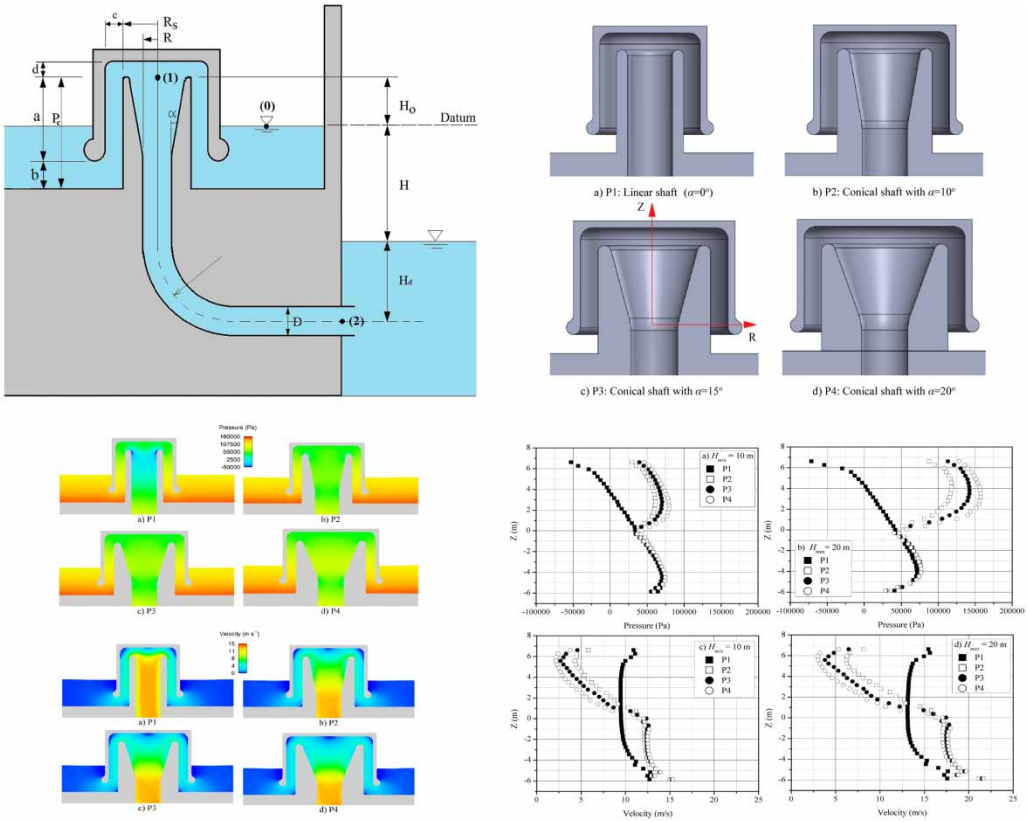

INTRODUCTION

Spillways can be grouped into controlled (gated) and uncontrolled (free overflow) spillways in general. Thanks to the controlled spillways, the water level can be adjusted precisely or kept constant above the crest level. Thus, a better reservoir operation can be achieved by minimizing the level changes in the reservoir. However, the biggest problem of this type of spillway is the maintenance, repair, and operating costs of the moving hydraulic elements, although they cannot be operated very often. In the other type, free overflow spillway, water is allowed to pass freely over a fixed spillway profile when it exceeds the crest level. However, since it is not possible to control the water level, large level changes occur during floods and thus an effective reservoir operation cannot be achieved. Siphon-shaft spillways can offer the advantages of these two spillway types together. Siphon-shaft spillways do not need any movable control elements, and water level changes in reservoirs do not affect the spillway discharge much. They also have the capability to sluice below the crest level (like bottom outlets). Thus, more effective flood control can be achieved in the reservoir when necessary. Since siphon-shaft spillways are placed inside the reservoir, they can be used safely even in embankment and arch dams where spillways have a placement problem. However, it is still recommended to build a free overflow second spillway due to the operating modes and limited capacities of these spillways. One of the most important problems to be considered in the design of these spillways is cavitation. Siphon vacuum pressures need to be controlled and therefore their operating heads are limited. Another problem is limited sluice capacities.

The use of siphons in dam spillways has attracted the attention of researchers since the beginning of the 20th century. Davis & Stickney (1914), Stickney (1922), and Lawaczeck (1930) developed different siphon designs for dam spillways. Rousselier & Blanchet (1951), Head (1971), Charlton (1971), Ackers & Thomas (1975), Head (1975), Unser (1975), Ali & Pateman (1980), Ervine & Oliver (1980), and Bollrich (1994) conducted various theoretical and experimental studies on the design and performance of siphon spillways. Since the beginning of the 21st century, many researchers have tried to determine the performances by analyzing siphon spillways in different designs and hydraulic conditions with experimental and numerical methods (Babaeyan-Koopaei

et al. 2002; Houichi *et al.* 2006; Yücel 2008; Jourabloo 2010; Ghafourian *et al.* 2011; Musavi-Jahromi 2011; Tadayon & Ramamurthy 2013; Aydın *et al.* 2015; Petaccia & Fenocchi 2015).

Although there are many studies on both siphon and shaft spillways, there are limited studies on siphon-shaft type spillways, as a hybrid spillway. The idea of equipping a shaft spillway with a siphon was first put forward by Iyer (V.G.) in 1933–1934 in order to rapidly increase and maximize the flow of a shaft spillway. Later, Binnie (1938) applied a siphon to a bell-mouthed shaft spillway. This type of spillway, which will be called siphon-shaft, was first applied at Marconahali (India) dam and then again at Hirebhasagar dam in India. Binnie (1938) conducted experiments on the siphon-shaft weir that he created by adding a hood to the shaft weir to be used as a spillway in the existing diversion tunnel. Ağıralioğlu (1977) suggested that the section above the cavitation critical height could be enlarged in order to reduce vacuum pressures in high-head siphon-shaft weirs. Khatsuria (2005) pointed out that some precautions must be taken to prevent the formation of cavitation by vacuum pressures in a siphon spillway. Aydin & Ulu (2021) studied the aeration performance of the aeration holes to prevent cavitational pressures based on the idea of Ağıralioğlu & Müftüoğlu (1989). This study focuses on the enlargement effect of the siphon-shaft profiles on the vacuum pressures in the shaft, which is able to trigger cavitation. Aydın & Ulu (2023a), inspired by Ağıralioğlu (1977), developed a pressure-controlled siphon-shaft spillway profile based on Bernoulli's principle. A disadvantage of this profile, which can adjust cavitation pressures very effectively, is that it creates a large footprint. In this study, the aim is to examine the expansion effect at the shaft mouth by using linear profiles instead of non-linear profiles (Wagner's profile and the pressure-controlled profile offered by Aydın & Ulu (2023a)). For this, some conical profiles with different enlarging angles were applied to a siphon-shaft spillway and their effects on cavitation pressure and discharge performance were investigated.

SHAFT PROFILES

According to the nappe head on the crest, the spillway flow is controlled by three different flow conditions: free flow, submerged, and full orifice. In all three cases, hydraulic sections do not operate at full capacity due to effects such as swirling, vibration, turbulence, and air intake. The hydraulic performance of shaft spillways depends on the hydraulic profile at the entrance of the shaft. While using the Wagner profile that fits the free flow jet suggested by USBR on a solid shaft spillway, crest shapes such as daisy, labyrinth, and piano-key were also tried in addition to morning-glory in order to increase the discharge capacity (Aydin & Ulu 2023b). Siphon-shaft spillways, which are formed by covering the top of the shaft spillways with a hood and operating them with the siphon effect, can be operated with pressure and full hydraulic capacity even at low water heads or reservoir levels below the crest. However, the low siphonic pressures of these spillways must be kept under control. For this purpose, a shaft profile specifically for siphon-shaft spillways was first developed by Aydın & Ulu (2023a). Developed based on the Bernoulli principle, this pressure-controlled siphon-shaft profile offers a very effective performance in terms of high discharge and pressure control, while giving a wide footprint.

USBR (1987) defined the profiles for the shaft (bell-mouth or morning-glory) spillways in free-flow conditions based on Wagner (1956). The crest and transition zone profile fitted to the lower nappe of the free overflow of a sharp-crested circular weir is shown in Figure 1.

In this study, a contracting cone with fixed wall angles was designed for the shaft mouth to dismiss the vacuum pressures inside the shaft (Figure 2). Three different coning angles ($\alpha = 10°$, 15°, and 20°) were applied to the cone in the shaft mouth together with a linear shaft profile ($\alpha = 0°$, Aydın & Ulu 2023a). The cases with coning angles of 0°, 10°, 15°, and 20° will be called P1, P2, P3 and P4, respectively (Figure 3). The main purpose of these profiles is to increase the pressure by increasing the flow cross-section toward the crest where the siphon pressure is the lowest. In the applied model in Figures 2(a)–2(d) are the geometric parameters of the siphon-shaft, H is the operating head (difference between the upstream head and downstream head), H_d is the piezometric head at the outlet, H_o is the crest height from the upstream water surface, R_s is the radius of the shaft mouth, R is the shaft outlet radius, P_c is the crest height from the reservoir bottom. While the upstream water level in the reservoir was variable, the tail-water level at the spillway outlet was kept constant under a certain piezometric head (H_d) to ensure the full siphon action. $R = 2.00$ m, $D = 4.00$ m, $H_d = 6.00$ m, $a = 7.58$ m, $b = 1.62$ m, $c = 1.50$ m, $d = 1.52$ m were taken as constant. The sharp edges adjacent to the flow were hydraulically rounded with a curve radius of 4 m to prevent separation zones

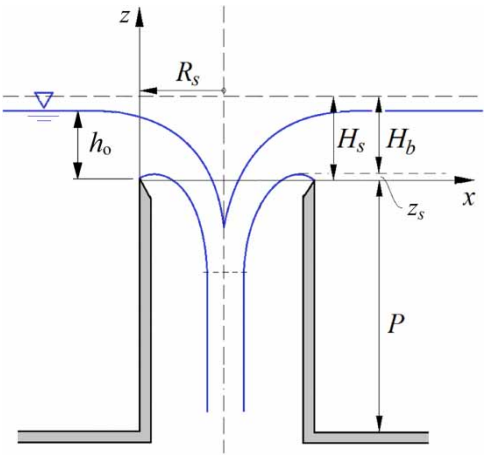

Figure 1 | Free overflow on a sharp-crested shaft weir (modified from USBR 1987).

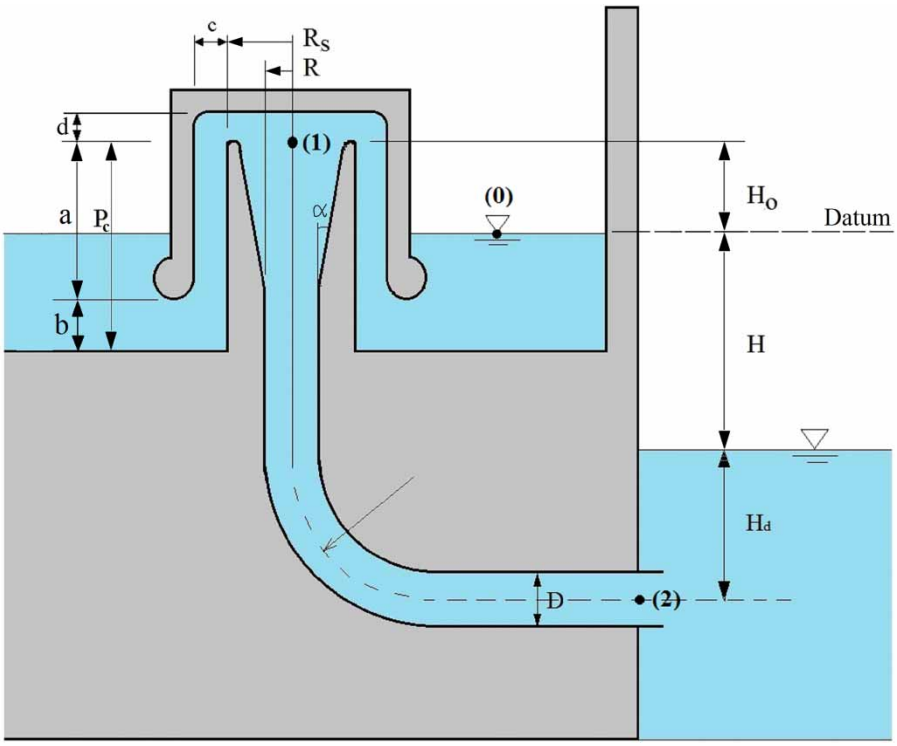

Figure 2 | Model definition of siphon-shaft spillways with a conical enlarging shaft.

in flow. The operating head is taken into account as a variable in the range of $H = 10$–20 m and R_s is taken as 3.0, 4.18, 4.80, and 5.44 m (from P1 to P4 case), respectively, depending on the coning angle.

METHOD

Computational fluid dynamics (CFD) has attracted attention as a powerful modeling and computational technique in recent years and has been widely used in many areas such as hydraulics, mechanics, industry, environment, automotive, and aerospace where fluid movements are important. CFD was tested many times by the researchers and has been successfully used in their hydraulic model studies, i.e. open channel, weirs, and spillway models (Musavi-Jahromi 2011; Tadayon & Ramamurthy 2013; Aydin *et al.* 2015, 2019, 2020, 2022; Aydin & Isik 2015; Aydin 2016a, 2016b; Parsaie *et al.* 2016; Aydin & Ulu 2021, 2023a, 2023b). FLOW-3D which is a general-purpose CFD software uses the finite volume method as a discretization method to

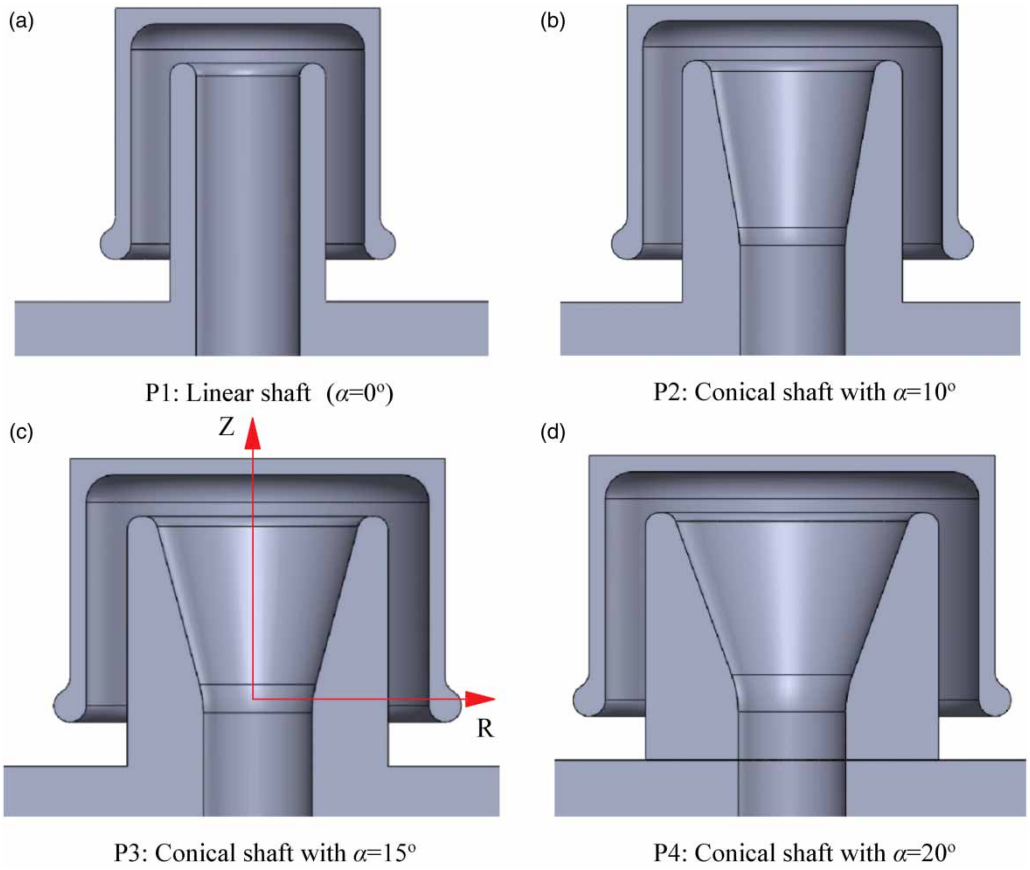

Figure 3 | Solid models for different conical shaft profiles.

solve the following governing equations in three dimensionless Cartesian coordinates for incompressible single-phase fluid flows.

$$\frac{\partial}{\partial X_i}(U_i A_i) = 0 \tag{1}$$

$$\frac{\partial U_i}{\partial t} + \frac{1}{V_F}\left[U_j A_j \frac{\partial u_i}{\partial X_j}\right] = -\frac{1}{\rho}\frac{\partial P}{\partial X_i} + G_i + f_i \tag{2}$$

where t refers to the time, ρ refers to the fluid density, V_f refers to the volume fraction open to flow, U_i indicates the mean velocity vectors, P is the hydrostatic pressure, A_i is the fractional area open to the flow in i direction, G_i is the mass acceleration, f_i is the viscous acceleration or Reynolds stress. The Volume of Fluid (VOF) estimates the interface in free-surface flows described by Hirt & Nichols (1981) for Cartesian coordinates as follows.

$$\frac{\partial F}{\partial t} + \frac{1}{V_F}\left[\frac{\partial}{\partial x}(FA_x u) + \frac{\partial}{\partial y}(FA_y v) + \frac{\partial}{\partial z}(FA_z w)\right] = 0 \tag{3}$$

Here, F represents the volume fraction occupied by the fluid for a single fluid. Physically, the voids represent regions of very low density compared to liquid, such as air. A modified volume of fluid method (TruVOF) is used in the free-surface tracking based on the VOF formulation. The k–ε turbulence model which is prepared in the solutions consists of two transport equations for the turbulent kinetic energy and its dissipation (Flow-Science 2019). As an application on the CFD on the scope, Aydin *et al.* (2015) successfully analyzed the hydrodynamics of a siphon side weir using a CFD technique. All the CFD simulations were carried out according to the flow chart in Figure 4.

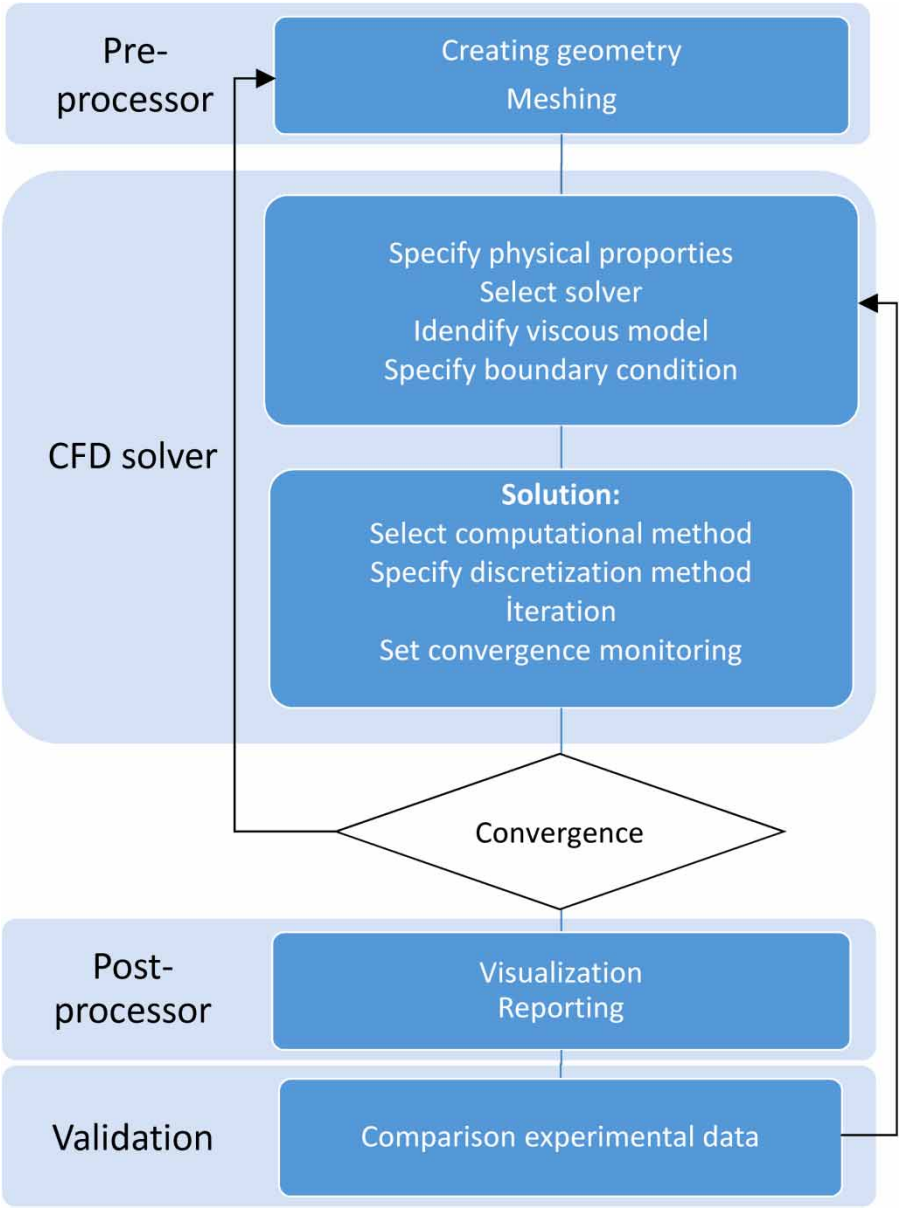

Figure 4 | Flow chart for CFD simulation.

Numerical accuracy

Ağıralioğlu (1977) conducted a series of physical model studies in a hydraulic laboratory to develop a head shape for a siphon-shaft spillway and to verify the mathematical model results he obtained. Some data of this experimental model are used as a benchmark (for $c = 75$, $a = 160$, $d = 110$ mm) to validate the numerical model. In the benchmark model, the shaft profile was described based on the USBR (1987) design principles for the submerged flow condition of the shaft spillway. A standard profile (Wagner profile) was applied to the shaft entrance in order to keep the head dimensions small. Since the shaft inlet is always full during a siphonic flow, it was stated that it would be appropriate to determine the shaft inlet profile according to the submerged state of sharp-edged shaft weirs. The shaft profile for the physical model was obtained from Wagner (1956) tables for $Q = 60$ l/s, $R_s = 0.16$ m, $H_o = 0.12$ m, $P_c = 0.32$ m, operating head $H = 0.124$ m, and $H/R_s = 0.775$. The shaft diameter (D) was obtained as $D = 0.18$ m by trial and error, assuming 75% full at the flow rate at the project operating head, so that the difference between the crest level and the base outlet elevation was 1.0 m. According to the recommendation of USBR (1987), the radius of curvature of the elbow was chosen greater than 1.5 times the diameter of the gallery, and the radius of curvature of the inner wall was taken as $2D = 0.36$ m and thus the radius of curvature of the elbow center was taken as 0.45 m.

The discharge of the siphon-shaft spillways can be calculated by the following equation.

$$Q = C_o A_o \sqrt{2gH} \tag{4}$$

where Q is the spillway discharge, A_o is the area of outlet galley, g is the gravitational acceleration, H is the operating head. The relative errors between the CFD and the experimental model (Benchmark) data were in the range of 1.2–4.4% for the flow discharges (Figure 5(a)), and 4.5–7.5% for the discharge coefficients (Figure 5(b)). These results indicate that the numerical model results have sufficient reliability.

An uncertainty analysis, Grid Convergence Index (GCI), was also performed to reveal the grid sensitivity on the numerical solutions based on the ASME procedure (Roache *et al.* 1986; Freitas 1993; Celik *et al.* 2008). Three grid sizes (fine, medium, and coarse grids) were applied to the numerical domain with a grid refinement factor of 1.4. The maximum numerical uncertainty for the velocity profiles in the fine-grid solution was reported as 0.16%, which corresponds to ± 0.0026 m/s for the centerline, and 3.1%, which corresponds to 0.052 m/s. The global average of the local order of accuracy was determined as 18.02 for shaft-centerline and 8.01 for shaft-edge, which indicates good calculations. The maximum relative errors are 0.8 and 2.8%, respectively. It can be noticed that all uncertainties are within reasonable limits with respect to the grid size.

Hydraulic performance of shaft profiles

Prototype-scale 3D CFD models were used to determine the hydrodynamic properties of siphon-shaft spillway flows for different cases (P1–P4). Figure 6 shows the pressure contours of the siphonic flow for the minimum operating head ($H = 10$ m). The lowest pressures occur at the shaft crest and in the shaft transition region (at the edge points where the contraction stops). In the P2–P4 profiles, the siphonic pressures dismiss significantly, especially at the critical shaft crest. This also indicates that the risk of cavitation is significantly reduced. Figure 7 presents the velocity contours to evaluate the hydraulic efficiency of the profiles. As the conical angle increases, the velocities above the shaft decrease, which means that the pressures decrease. The stagnation zones in the inner middle and sides of the hood reduce the hydraulic performance of the flow. Therefore, the section with rounded edges can be improved in terms of hydraulics performance, but this is beyond the scope of this study.

It is important to observe the pressure and velocity distributions in the regions close to the spillway surfaces to control the cavitation. The plots in Figure 8 illustrate pressure and velocity distributions near the shaft walls in the siphonic flow in more detail. As seen in Figures 8(a) and 8(b), while the linear profile (P1) causes a decreasing pressure distribution in the shaft upwards, the conical profiles (P2–P4) provide significant increases in pressures toward the crest from $Z = 0$ which indicates transition edge. This increase in conical shafts is more pronounced at a maximum operating head (Figure 8(b)). The P1 profile exposes the upper critical areas of the shaft to low vacuum pressures that are risky for cavitation, but the conical profiles significantly increase the pressures in the critical region, removing them from cavitation pressures. At a low operating head ($H = 10$ m), the minimum pressure for P1 is -53 KPa, and 30, 34, and 37 KPa for P2, P3, and P4, respectively. The average pressures are 28,

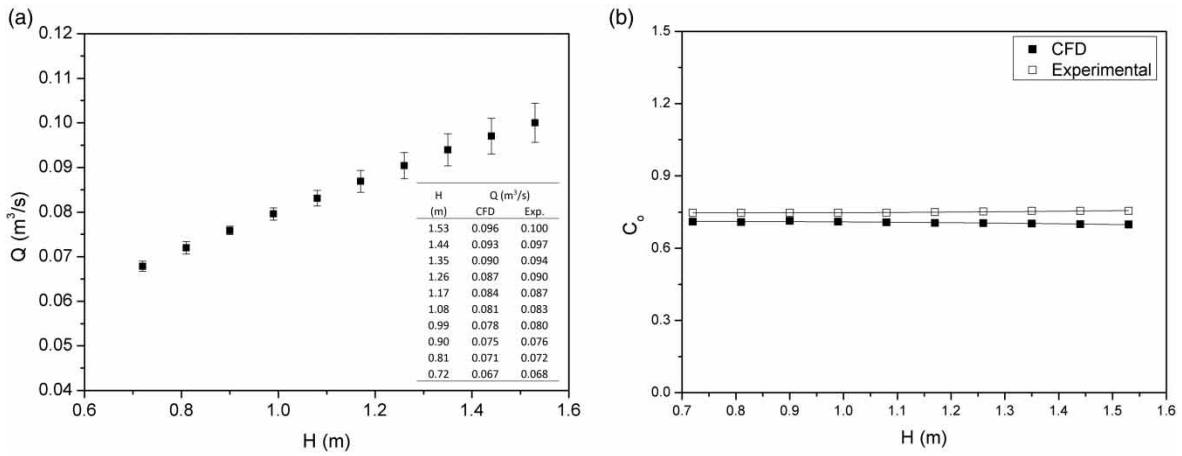

Figure 5 | Comparison of experimental and numerical model results: (a) spillway discharges with relative error bars and (b) discharge coefficients.

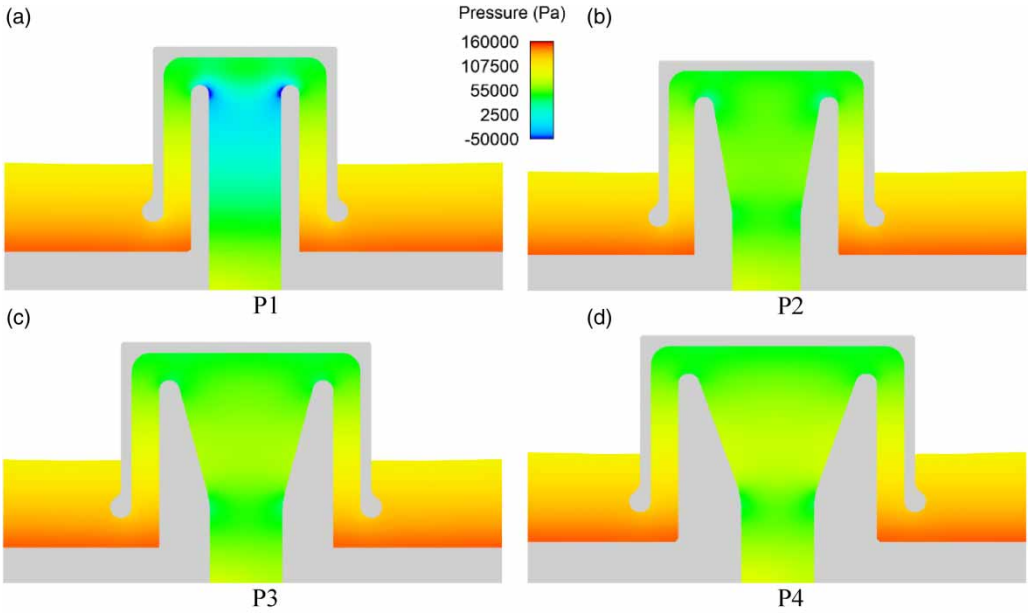

Figure 6 | Pressure contours in siphonic flows with different coning angles.

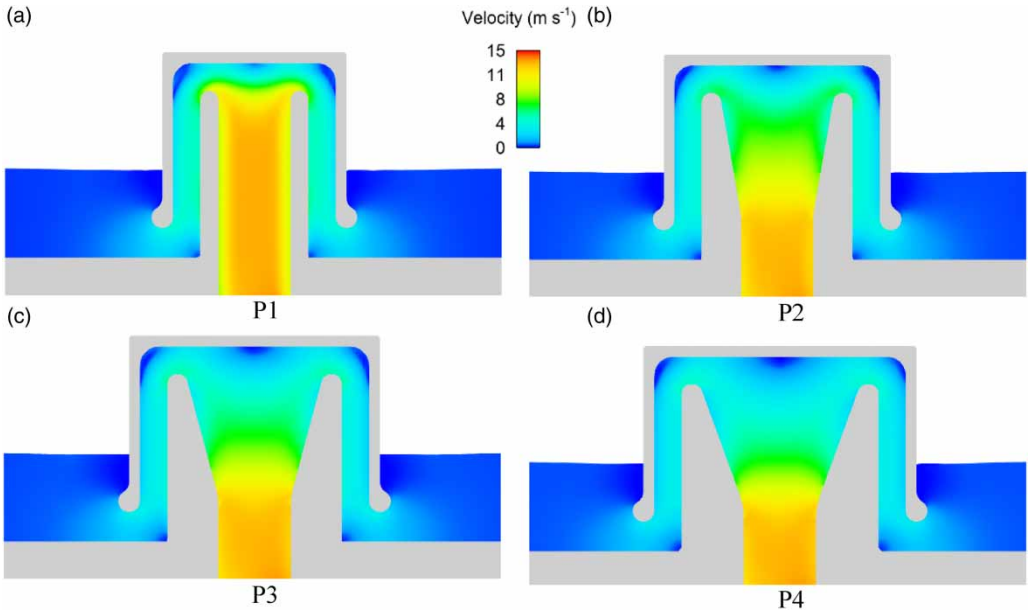

Figure 7 | Velocity contours in siphonic flows with different coning angles.

56, 58, and 64 KPa for P1, P2, P3, and P4, respectively. For $Z \geq 0$, the average of 7–9 times increase in pressures in the shaft was determined with conical profiles (P2–P4) for the low operating head. These increases are up to 11–15 times at the high operating head.

In Figures 8(c) and 8(d), the velocity distributions near the shaft surface are given for the minimum and the maximum operating heads, respectively. As seen in these plots, the conical profiles reduce flow velocities toward the crest from 15 to 2 m/s for $H_{min} = 10$ m, and from 20 to 3 m/s for $H_{max} = 20$ m. The average decreases in flow velocities are between 25 and 50% with P2–P4 conical profiles for $Z \geq 0$. For $Z < 0$, an average increase of 20–25% was observed at the velocities in the shaft due to the increase in the discharge capacity with the conical profiles. In general, the coning angle has an increasing effect on the pressure distribution and a decreasing effect on the velocity distribution along the conical shaft. These effects are more pronounced for high operating heads (Figure 8).

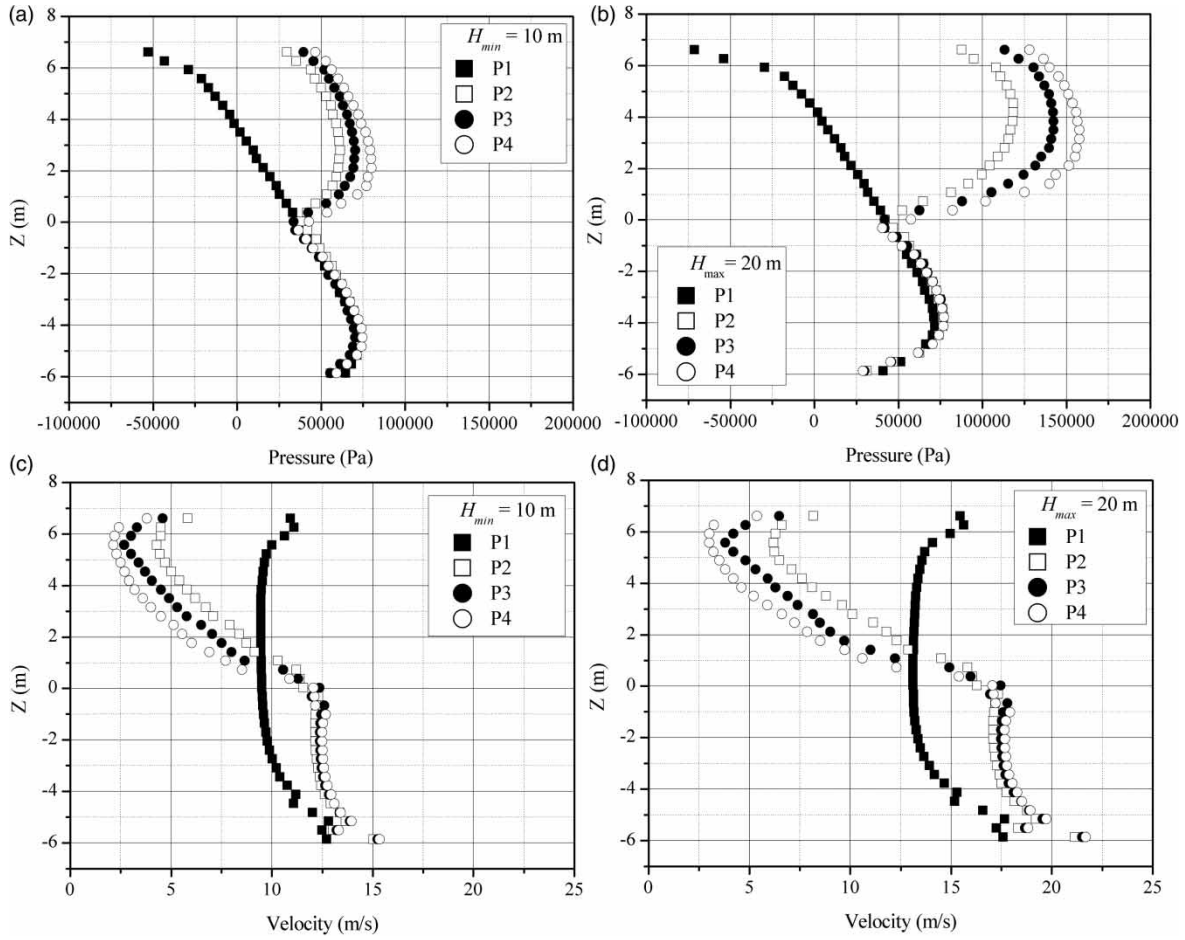

Figure 8 | Pressure and velocity distributions near shaft wall for minimum and maximum operating heads.

A cavitation index including the pressure and velocity parameters should be calculated to determine the cavitation potential within the shaft. Falvey (1990) presents cavitation numbers as follows.

$$\sigma = \frac{P - P_v}{\rho U^2/2} \tag{5}$$

where P refers to the reference absolute pressure, P_v refers to the absolute vapor pressure of water, ρ refers to the density of water, U refers to the flow velocity in the cavitation zone. At the water temperature of 20 °C, $\rho = 998.2$ kg/m^3 and $P_v = 2330$ Pa. Although cavitation can theoretically start when the pressure drops below the vapor pressure at a normal water temperature, it can start at higher pressure due to dissolved gas and/or particles in suspension. On the other hand, it may occur even at unexpected average pressures due to pressure fluctuations in turbulent flows (Novak *et al.* 2007). In the abstract, it is considered that cavitation is not formed when the cavitation number is greater than 1.0. However, the critical value may be smaller than this value because of friction, irregularities in the flow pattern. According to Ağiralioğlu (1977), in practice, the critical cavitation index at which cavitation begins is considered to be 0.7. This value corresponds to 7 m of water column. The USBR (1987) recommends the sub-atmospheric (vacuum) pressure at the crest to be 6.70 m for sea level to avoid cavitation. Houichi *et al.* (2006) also defined this limit value as 7.92 m for the siphon crest at sea level. Time-dependent pressure fluctuations can also generate cavitation due to high turbulence or eddies/vortices formation in the flow (Tullis 1989).

Figure 9 presents the variation of the cavitation number calculated by Equation (5) along the shaft near the solid surface. For $Z > 0$, it is seen that the conical profiles have a significant increasing effect on the cavitation number, but for $Z < 0$, the cavitation numbers are around the critical value. For $Z \geq 0$ and $H = 10$ m, the cavitation number increases on average from 0.01 of P1 to 2.59–10.85 with the use of P2–P4, respectively. This increase

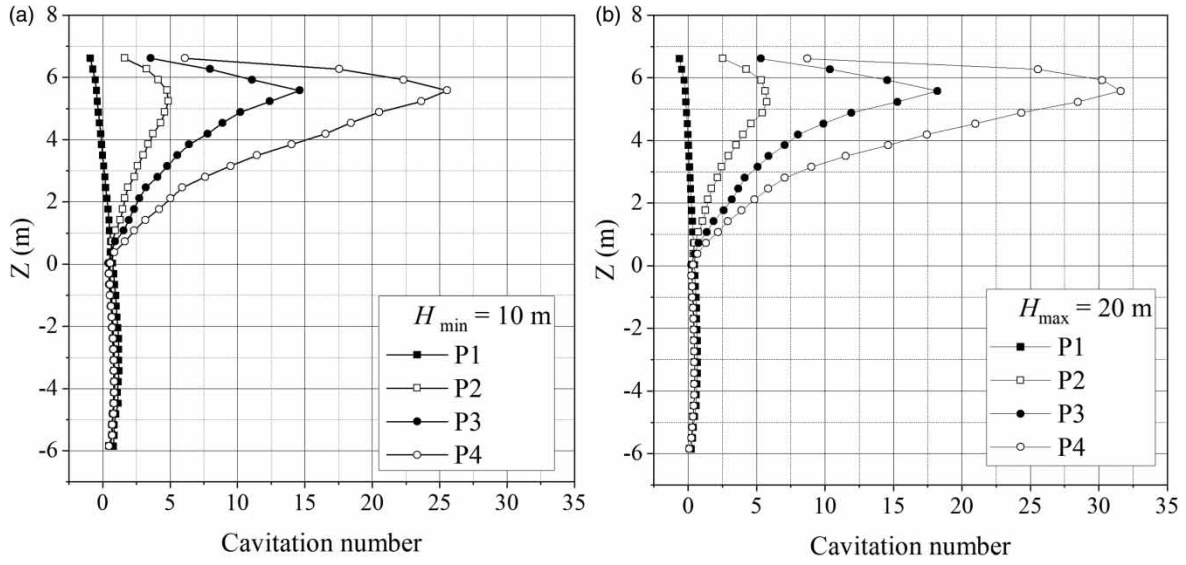

Figure 9 | Variations of cavitation number along shaft profiles for different cases at (a) minimum operating head and (b) maximum operating head.

is from 0.05 to 2.81–12.58 with P2–P4, respectively, for $H = 20$ m. Cavitation numbers at the crest, which is the most critical point with respect to cavitation, increase from $\sigma = -0.92$ of P1 at minimum operating head to $\sigma = 1.63$, $\sigma = 3.57$ and $\sigma = 6.12$ for P2, P3, and P4, respectively. The cavitation numbers increase up to 4.86–25.57 for H_{min} and 5.76–31.59 for H_{max} around the shaft mouth (Z = 5.5 m). These values prove that the conical profiles (P2–P4) expanding toward the crest eliminate the risk of cavitation in the shaft. On the other hand, there is no significant change in the down regions of the shaft ($Z < 0$) that are exposed to lower cavitation pressures. In order to eliminate the risk of vacuum pressures in corners in the shaft and hood, attention should be paid to the flow separation of these regions.

Figure 10(a) shows the discharge capacity of the siphon-shaft spillway for the different cases. The discharge performance linearly increases with the operating head. The discharge capacity significantly increases for conical profiles (P2–P4) relative to the P1 profile. Also seen in Figure 10(b), the discharge coefficients for each case are almost constant versus the relative operating head (H/D). With this capacity increase, the discharge coefficient of the siphon-shaft spillway increases from the average $C_o = 0.81$ to 0.89, 0.90, and 0.91, respectively. The increase in the discharge performances on an average is 10, 11, and 12% for P2, P3, and P4, respectively. The linear-expanding P2–P4 profiles presented in this study offer a discharge performance close to that of the non-linear pressure-controlled profile presented by Aydın & Ulu (2023a) (about $C_o = 0.92$).

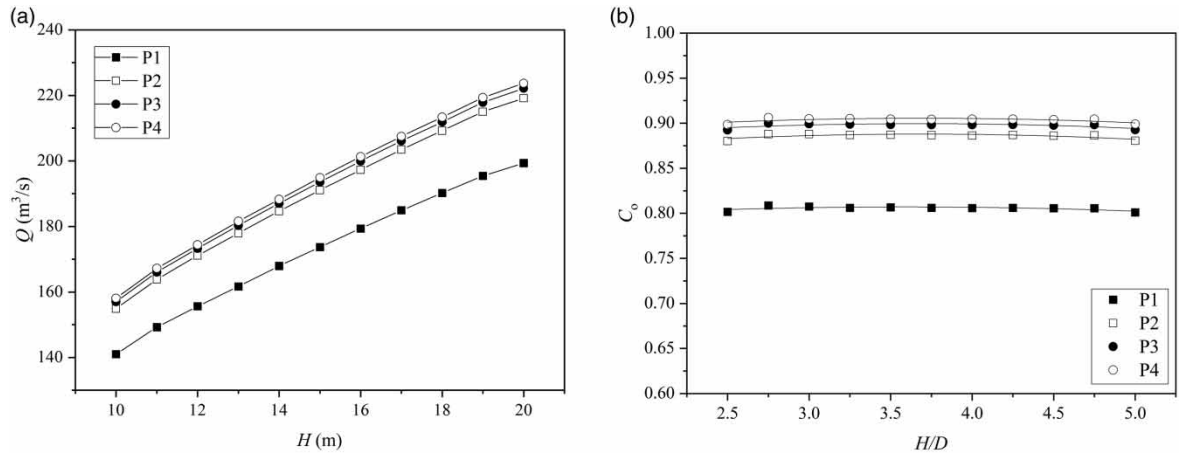

Figure 10 | Discharge performances for different cases: (a) head–discharge relationships and (b) discharge coefficients versus relative operating head.

CONCLUSIONS

This study focuses on the effect of a linear expanding shaft profile (conical shaft) on the hydraulic performance of siphon-shaft spillways. For this purpose, conical shaft profiles with three different coning angles were used together with a linear shaft profile. The prepared models were analyzed with a three-dimensional CFD technique, the accuracy of which was tested by a reliable procedure in the literature. In the model calibration tests, the results of the CFD models showed a maximum deviation of 4.4% from the experimental results in terms of spillway discharges. The maximum grid uncertainty for the velocity profiles was calculated as 3.1%, which corresponds to an edge velocity of ± 0.052 m/s. Numerical analysis details are shown that increasing the coning angle significantly decreases the vacuum pressures and velocities in the siphon-shaft. Therefore, it is noted that the use of conical shaft mouths in siphon-shaft spillways significantly reduces the risk of cavitation, as well as increasing discharge performance. It also provides an average 11% increase in discharge efficiency. In addition, it can provide economy thanks to a lower footprint, but attention should be paid to the streamlining capability due to sudden turns in the transition sections. In terms of better hydraulic efficiency, the pressure-controlled profile developed for siphon-shaft spillways by Aydın & Ulu (2023a) may be a more suitable option despite a larger footprint. It should also be stated that this study was carried out under certain limitations with three different cone angles ($0 \geq \alpha \geq 20°$), an operating head range of $10\text{ m} \geq H \geq 20\text{ m}$, and a shaft diameter of $D = 4$ m. It is recommended to carry out a detailed hydraulic modeling study where dimensionless parameters will be applied so that the study can be applied to different dimensions and hydraulic conditions.

ACKNOWLEDGEMENTS

This study was supported by the Scientific and Technological Research Council of Turkey (TUBITAK) with the project No. 219M006.

DATA AVAILABILITY STATEMENT

All relevant data are included in the paper or its Supplementary Information.

CONFLICT OF INTEREST

The authors declare there is no conflict.

REFERENCES

Ackers, P. & Thomas, A. R. 1975 Design and operation of airregulated siphons for reservoir and head-water control. In *Symp. Design and Operation of Siphons and Siphon Spillways*. BHRA Fluid Engineering, UK, pp. A1.1–A1.20.

Ağıralioğlu, N. 1977 *Sifonlu Şaft Savaklarda Akım Durumunun Etüdü ve Başlık Şeklinin Geliştirilmesi (Study of Flow Situation in Siphon Shaft Weirs and Development of Head Shape)*. PhD Dissertation, *İstanbul Teknik Üniversitesi*. İnşaat Fakültesi, İstanbul, Türkiye.

Ağıralioğlu, N. & Müftüoğlu, F. 1989 Hood characteristics for Siphon-Shaft spillways. *Journal of Hydraulic Engineering.* **115** (5), 636–649.

Ali, K. & Pateman, D. 1980 Theoretical and experimental investigation of air-regulated siphons. *Proceedings of the Institution of Civil Engineers Part 2* **69** (1), 111–138.

Aydin, M. C. 2016a Investigation of a sill effect on rectangular side-weir flow by using CFD. *Journal of Irrigation and Drainage Engineering* **142** (2), 04015043.

Aydin, M. C. 2016b New approach for estimation of rectangular side weirs discharge in subcritical flow. *Journal of Irrigation and Drainage Engineering* **142** (5), 04016012.

Aydin, M. C. & Isik, E. 2015 Using CFD in hydraulic structures. *International Journal of Scientific and Technological Research* **1** (5), 7–13.

Aydin, M. C. & Ulu, A. E. 2021 Aeration performance of high-head siphon-shaft spillways by CFD models. *Applied Water Science* **11** (10), 1–12.

Aydin, M. C. & Ulu, A. E. 2023a Developing and testing a novel pressure-controlled hydraulic profile for siphon-shaft spillways. *Flow Measurement and Instrumentation* **90**, 102332.

Aydin, M. C. & Ulu, A. E. 2023b Numerical investigation of labyrinth-shaft spillway. *Applied Water Science* **13** (4), 89.

Aydin, M. C., Ozturk, M. & Yucel, A. 2015 Experimental and numerical investigation of self-priming siphon side weir on a straight open channel. *Flow Measurement and Instrumentation* **45**, 140–150.

Aydin, M. C., Ulu, A. E. & Karaduman, C. 2019 Investigation of aeration performance of Ilısu Dam outlet using two-phase flow model. *Applied Water Science* **9** (4), 1–13.

Aydin, M. C., Isik, E. & Ulu, A. E. 2020 Numerical modeling of spillway aerators in high-head dams. *Applied Water Science* **10** (1), 1–9.
Aydin, M. C., Aytemur, H. S. & Ulu, A. E. 2022 Experimental and numerical investigation on hydraulic performance of slit-check dams in subcritical flow condition. *Water Resources Management* **36** (5), 1693–1710.
Babaeyan-Koopaei, K., Valentine, E. M. & Alan Ervin, D. 2002 Case study on hydraulic performance of Brent Reservoir siphon spillway. *Journal of Hydraulic Engineering* **128** (6), 562–567.
Binnie, G. M. 1938 Model experiments on bellmouth and Siphon-Belmouth overflow spillways. *Journal of the Institution of Civil Engineers* **10** (1), 65–90.
Bollrich, G. 1994 Hydraulic investigations of the high-head siphon spillway of Burgkhammer. In: *ICOLD 18th Congress*. International Commission on Large Dams, Paris.
Celik, I. B., Ghia, U., Roache, P. J., Freitas, C. J., Coleman, H. & Raad, P. A. 2008 Procedure for estimation and reporting of uncertainty due to discretization in CFD applications. *ASME Journal of Fluids Engineering* **130** (7), 078001.
Charlton, J. A. 1971 The design of air-regulated spillway siphons. *Journal of the Institution of Water Engineers* **25** (6), 325–336.
Davis, W. R. & Stickney, G. F. 1914 *Siphon Spillway, Patent No: 1,0083,995*. United States Patent Office.
Ervine, D. A. & Oliver, G. C. S. 1980 The full scale behaviour of air-regulated siphon spillways. *Proceedings of the Institution of Civil Engineers, Part 2* **69**, 687–706.
Falvey, T. F. 1990 *Cavitation in Chutes and Spillways*. Bureau of Reclamation, Engineering Monograph. No.42, United State Department of The Interior, Denver, CO.
Flow Science 2019 *FLOW-3D User Manual*. Theory, Flow Science, Inc, Santa Fe, NM.
Freitas, C. J. 1993 Journal of fluids engineering editorial policy statement on the control of numerical accuracy. *Journal of Fluids Engineering* **115**, 339–340.
Ghafourian, A., Mousavijahromi, H. & Shafaee Bajestan, B. 2011 Hydraulic of siphon spillway by physical and computational fluid dynamics. *World Applied Sciences Journal* **14** (8), 1240–1245.
Head, C. R. 1971 A self-regulating river siphon. *Journal of the Institution of Water Engineers* **25** (1), 63–72.
Head, C. R. 1975 Low-head air-regulated siphons. *Journal of the Hydraulics Division* **101** (3), 329–345.
Hirt, C. W. & Nichols, B. D. 1981 Volume of fluid (VOF) method for the dynamics of free boundaries. *Journal of Computational Physics* **39** (1), 201–225.
Houichi, L., Ibrahim, G. & Achour, B. 2006 Experiments for the discharge capacity of the siphon spillway having the Creager-Ofitserov profile. *International Journal of Fluid Mechanics Research* **33** (5), 395–406.
Jourabloo, M. 2010 *Investigation of Hydraulic in Siphon Spillway*. Islamic Azad University, Tehran.
Khatsuria, R. M., 2005 *Hydraulics of Spillways and Energy Dissipators* (Meyer, M. D., ed.). Marcel Dekker, New York.
Lawaczeck, F. 1930 *Siphon Spillway, Patent No: 1,770,340*. United States Patent Office.
Musavi-Jahromi, S. H. 2011 Simulation of pizometric pressure in dam Siphon spillway. *World Applied Sciences Journal* **12** (7), 1074–1083.
Novak, P., Moffat, A. I. B., Nalluri, C. & Narayanan, R. 2007 Dam Outlet Works. In: *Hydraulic Structures* (P. Novak, A.I.B. Moffat, C. Nalluri, R. Narayanan, eds.). Taylor & Francis, London, UK, pp. 153–176.
Parsaie, A., Dehdar-Behbahani, S. & Haghiabi, A. H. 2016 Numerical modeling of cavitation on spillway's flip bucket. *Frontiers of Structural and Civil Engineering* **10** (4), 438–444.
Petaccia, G. & Fenocchi, A. 2015 Experimental assessment of the stage–discharge relationship of the Heyn siphons of Bric Zerbino dam. *Flow MeasurementandInstrumentation* **41**, 36–40.
Roache, P. J., Ghia, K. N. & White, F. M. 1986 Editorial policy statement on control of numerical accuracy. *Journal of Fluids Engineering.* **108**, 1.
Rousselier, M. & Blanchet, P. 1951 Some realizations of siphons. In: *ICOLD 4th Congress*. International Commission on Large Dams, Paris.
Stickney, G. F. 1922 *Siphon Spillway, Patent No: 1,405,071*. United States Patent Office.
Tadayon, R. & Ramamurthy, A. S. 2013 Discharge coefficient for siphon spillways. *Journal of Irrigation and Drainage Engineering* **139** (3), 267–270.
Tullis, J. P. 1989 *Hydraulics of Pipelines, Pumps, Valves, Cavitation, Transients*. A Wiley – Interscience Publication, John Wiley & Sons, Inc., New York.
Unser, K. 1975 Design of low head siphon spillways. Symp. Design and Operation of Siphons and Siphon Spillways, BHRA Fluid Engineering, UK, C5.55–C5.68.
USBR 1987 United States Department of the Interior Bureau Reclamation. In: *Design of Small Dams* (H. G. Arthur & E. H. Larson, eds.). A Water Resources Technical Publication, Washington, DC.
Wagner, W. E. 1956 Morning-glory shaft spillways (a symposium): determination of pressure-controlled profiles. *Transactions of the American Society of Civil Engineers* **121**, 345–384.
Yücel, A. 2008 *Yan Savak Sifonlarındaki Akımın Kıvrımlı Bir Kanal Boyunca İncelenmesi (The Investigation of Side-Weir Siphons Flow Along a Curved Channel)*. PhD Dissertation. Fırat Üniversitesi Fen Bilimleri Enstitüsü, Elazığ, p. 192s.

First received 8 December 2022; accepted in revised form 5 May 2023. Available online 17 May 2023